RSC Advances

PAPER

View Article Online
View Journal | View Issue

Cite this: *RSC Adv.*, 2017, **7**, 55577

An acidic pH fluorescent probe based on Tröger's base

Chunxue Yuan, *[ab] Yanmin Zhang,[a] He Xi [c] and Xutang Tao [b]

Received 12th October 2017
Accepted 2nd December 2017

DOI: 10.1039/c7ra11228a

rsc.li/rsc-advances

A novel pH fluorescent probe 2,8-(6*H*,12*H*-5,11-methanodibenzo[*b*,*f*]diazocineylene)-di(*p*-ethenylpyridine) (**TBPP**) incorporating an electron-donating amine moiety and electron-accepting pyridine group through Tröger's base linker was designed and synthesized. **TBPP** exhibits an intramolecular charge transfer effect caused by the donor–acceptor interaction between its amine and pyridine units. Its emission can be reversibly switched between blue and dark states by protonation and deprotonation. Such behavior enables it to work as a turn-off fluorescent pH sensor in solution state. ^{1}H NMR spectroscopy analysis suggests that the change in electron affinity of the pyridinyl unit upon protonation and deprotonation is responsible for such sensing processes.

Introduction

pH is a key parameter in a wide range of fields such as environmental analysis, chemical process control, food production, medical diagnosis and life science.[1–6] Many important physiological processes of cells and organelles are also related to pH values.[7,8] Consequently, the measurement of pH is of great importance in the field of environmental, chemical, medical and life sciences. Many techniques have been used for measuring pH value including UV-vis absorbance spectroscopy,[9,10] fluorescence spectroscopy,[11,12] nuclear magnetic resonance[13,14] and electrochemistry.[15,16] Among these methods, fluorescent probes for pH detection have attracted much more attention due to their convenient operation, particularly high sensitivity, non-invasiveness and real-time detection.[17] Towards this end, many kinds of pH fluorescent probes have been explored including fluoresceins,[18,19] coumarins[20,21] and rhodamines[22,23] *etc.* However, most reported fluorescence pH probes are practical for near-neutral pH range while there are limited probes for monitoring pH changes in acidic organelles. And some pH probes still suffer from the severe excitation interference caused by a shorter Stokes shift. There is a great pressing need to develop fluorescent probes toward high sensitivity and large Stokes shift for monitoring acid physiological pH fluctuations.

Tröger's base (TB),[24] first synthesized in 1887, has gained steady interest in recent years because of its *C*2 symmetry, chirality, and rigid concave shape.[25,26] Our recent work indicated pyridinium salts based on TB display a special aggregation-induced emission (AIE) property that it is non-emissive in solution but exhibit strong fluorescence in solid state.[27,28] In addition, N-heterocyclic derivatives are ideal substances for use as hydronium ion indicators owing to the high sensitivity and the exceptionally rapid rates of proto transfer occurring in acid–base equilibrium process.[11,29,30] With this in mind, we designed and synthesized a new compound **TBPP** based on TB by introducing the pyridine electron-withdrawing group into TB framework. We expect that optical change could be achieved through the transformation between the neutral **TBPP** and non-fluorescence ionic pyridinium salt by protonation. Proton titration experiments indicated that **TBPP** can be used as a turn-off pH fluorescent probe for acidic pH detection with high sensitivity.

Experimental section

Materials and instrumentation

All commercially available chemicals were purchased from Adamas, Aldrich and TCI, and used as received without further purification except *N*-methyl pyrrolidone was dried over 3 Å molecular sieves. 2,8-Dibromo-6*H*,12*H*-5,11-methanodibenzo[*b*,*f*][1,5]diazocine was prepared according to literature procedures.[31]

^{1}H and ^{13}C NMR spectra were recorded on a Bruker AVANCE 400 spectrometer. The chemical shifts are reported in δ ppm with reference to residual protons and carbons of $CDCl_3$ (7.26 ppm in ^{1}H NMR and 77.16 ppm in ^{13}C NMR) and DMSO-d_6 (2.50 ppm in ^{1}H NMR and 39.52 ppm in ^{13}C NMR). Coupling constants *J* are given in hertz. Mass spectra was measured with a Bruker Daltonics micrOTOF-focus using the APCI-TOF method in the positive-ion mode in toluene. The UV-visible absorption spectra were measured on a TU-1800

[a]*College of Materials Science and Engineering, Tongji University, Caoan Road 4800, Shanghai 201804, P. R. China. E-mail: cxyuan@tongji.edu.cn*

[b]*State Key Laboratory of Crystal Materials, Shandong University, Shanda South Road 27, Jinan, 250100, P. R. China*

[c]*School of Advanced Materials and Nanotechnology, Xidian University, South Taibai Road 2, Xi'an 710071, P. R. China*

spectrophotometer using a quartz cuvette having 1 cm path length. The photoluminescence spectra were collected on a Hitachi F-4500 fluorescence spectrophotometer with a 150 W Xe lamp. Fluorescence quantum yields (Φ) were determined using quinine sulfate in 0.1 N sulfuric acid (Φ = 0.577) as standard.

Solvents were purified and dried according to standard procedures. Thin layer chromatography (TLC) was performed on glass plates coated with 0.20 mm thickness of silica gel. Column chromatography was performed using neutral silica gel PSQ100B.

General procedure for spectroscopic measurements

Stock solution of probe with a concentration of 1.0 mM was prepared in DMSO and the solution for spectroscopic determination was obtained by diluting the stock solution to 10.0 μM in DMSO. The metal ions were provided by NaCl, KCl, $CaCl_2$, $MgCl_2$, $CuCl_2\cdot 2H_2O$, $MnCl_2$, $CoCl_2\cdot 6H_2O$, $Ni(NO_3)_2\cdot 6H_2O$, $Cd(NO_3)_2\cdot 4H_2O$, $AlCl_3$, $Zn(NO_3)_2\cdot 6H_2O$, $Cr(NO_3)_2\cdot 9H_2O$. In the pH titrations experiments, the slight pH variations of the solutions were achieved by adding the minimum volumes of HCl (1.0 mM). Spectral data were recorded after each addition. The excitation wavelength was 340 nm. The resulting solution was shaken well and kept at room temperature for 30 min before taking its absorption and fluorescence spectra.

Synthesis of 2,8-(6*H*,12*H*-5,11-methanodibenzo[*b*,*f*] diazocineylene)-di(*p*-ethenyl-*N*-pyridine) (TBPP)

To a stirring of 2,8-dibromo-6*H*,12*H*-5,11-methanodibenzo[*b*,*f*] [1,5]diazocine (5.0 mmol, 1.9 g), 4-vinyl pyridine (20.0 mmol, 2.2 mL) and K_2CO_3 (20.0 mmol, 2.8 g) in *N*-methyl pyrrolidone (10 mL) was added tris(2-methylphenyl)phosphine (0.001 mmol, 0.003 g) and palladium acetate (0.001 mmol, 0.0023 g) as catalysts. The mixture was stirred at 130 °C for 10 h under N_2 atmosphere and monitored by TLC. After the reaction was finished, the reaction mixture was cooled to room temperature and extracted by CH_2Cl_2 for three times. Combined organic phase was washed with water for three times and dried over anhydrous $MgSO_4$. After evaporation of the solvent, the mixture was purified by a silica gel column chromatography (eluent: CH_2Cl_2/ethanol = 40/1 in the ratio of volume) to afford **TBPP** (1.22 g, 2.85 mmol) in 57% yield as a light yellow solid. Mp: 287.01 °C. ^{1}H NMR (300 MHz, $CDCl_3$), δ (ppm): 4.23 (d, 2H, J = 16.5 Hz), 4.35 (s, 2H), 4.74 (d, 2H, J = 16.8 Hz), 6.86 (d, 2H, J = 16.2 Hz), 7.09–7.19 (m, 6H), 7.26–7.30 (m, 4H), 7.35–7.39 (dd, 2H, J = 8.4 Hz), 8.53 (d, 4H, J = 6.0 Hz). ^{13}C NMR (75.47 MHz, $CDCl_3$), δ (ppm): 58.72, 66.91, 120.69, 125.08, 125.43, 125.75, 126.09, 128.13, 132.11, 132.51, 144.65, 148.71, 150.11. HR-MS (APCI, positive): [(M + H)$^+$] calcd for $C_{29}H_{24}N_4$, 429.2074; found 429.2461.

Results and discussion

Synthesis

As outlined in Scheme 1, compound **TBPP** was synthesized in moderate yield directly by Heck coupling reaction of 4-vinyl pyridine with 2,8-dibromo-6*H*,12*H*-5,11-methanodibenzo[*b*,*f*] [1,5]diazocine in the presence of a base and palladium catalyst.

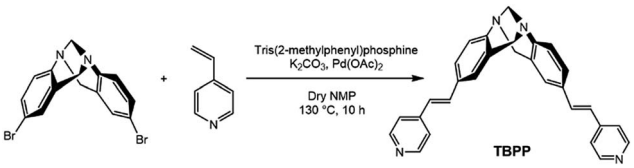

Scheme 1 Synthesis of probe TBPP.

The product was characterized by ^{1}H NMR, ^{13}C NMR and HRMS methods. It is readily soluble in normal solvents such as benzene, CH_2Cl_2, $CHCl_3$, THF, methanol, ethanol, CH_3CN, DMF, DMSO, but insoluble in hexane and water.

Photophysical properties of probe TBPP

In our experiment, we found that both of solutions and solids of **TBPP** show strong blue emissions (the photos were shown in the inset of Fig. 1(a)). The normalized absorption and fluorescence

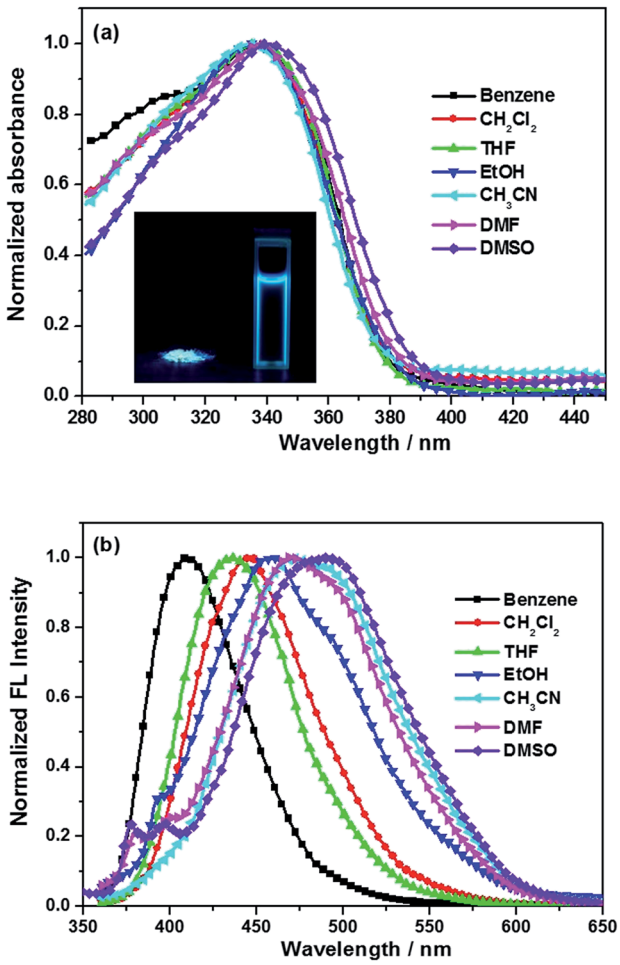

Fig. 1 Normalized (a) UV and (b) PL spectra of TBPP in solvents with different polarities. The inset shown the photos of the solutions and solids of TBPP under illumination. The excitation wavelength is 336 nm.

Table 1 Photophysical properties of TBPP

Solvent	λ_{abs}[a] (nm)	λ_F[b] (nm)	$\Delta\lambda$	Φ_F[c]
Benzene	335	409	74	0.74
CH_2Cl_2	337	445	108	0.94
THF	337	435	98	1.62
Ethanol	336	458	122	0.14
CH_3CN	336	473	137	0.50
DMF	337	472	135	0.94
DMSO	340	489	149	0.69

[a] Peak wavelength of absorption spectrum. [b] Peak wavelength of fluorescence spectrum. [c] Quantum yield determined using quinine sulfate as the standard.

emission spectra of **TBPP** in various solvents with different polarity were shown in Fig. 1. The absorption peak wavelength, fluorescence peak wavelength, Stokes' shift and fluorescence quantum yields were summarized in Table 1. Increase the polarity of solvent (benzene, CH_2Cl_2, THF, ethanol, acetonitrile, DMF, DMSO), no obvious spectral shift was observed in the absorption spectra with the absorption peaks locate at the range from 335 to 340 nm while fluorescence spectra shown a large red-shift that the fluorescence peaks changed from 409 to 489 nm. The Stokes' shift is changed from 74 nm to 149 nm. This can be explained by the fact that the excited state of the compound **TBPP** may possess higher polarity than that of the ground state. For the solvatochromism is associated with the energy level lowering. Increased dipole–dipole interaction between the solute and solvent leads to lowering the energy level greatly.[32,33] The amine on TB bridge and pyridine group act as electron donor and acceptor, respectively. Each wing of compound **TBPP** is a D–π–A charge transfer structure. Therefore, the intense fluorescence of **TBPP** in solution and solid state should contributed from the effective intramolecular charge transfer (ICT) through strong push–pull interaction between the electron-donor amine moiety on TB bridge and the electron-acceptor pyridine group.

pH titrations of probe TBPP

To study the optical responses of probe **TBPP** to pH, pH titrations of absorption spectra and fluorescence emission spectra were performed. As shown in Fig. 2(a), along with the H^+ addition, the original absorption band at 340 nm decreased and a new band around 390 nm increased gradually. A well-defined isosbestic point at 356 nm was observed. A notable color change from colorless to yellow (the inset in Fig. 2(a)) was observed upon increasing the acidity. Therefore, this probe can serve as a "naked-eye" colorimetric indicator for acidic pH.

The fluorescence property of **TBPP** as a function of pH were displayed in Fig. 2(b) and (c). Before the addition of acid, DMSO solution of **TBPP** exhibited an intense emission band around 490 nm with a large Stokes shift of 149 nm.[29,30,34,35] The large Stokes shift should help to reduce the excitation interference. Upon increasing the amount of H^+, the fluorescence intensity reduced gradually until quenched completely. The fluorescence

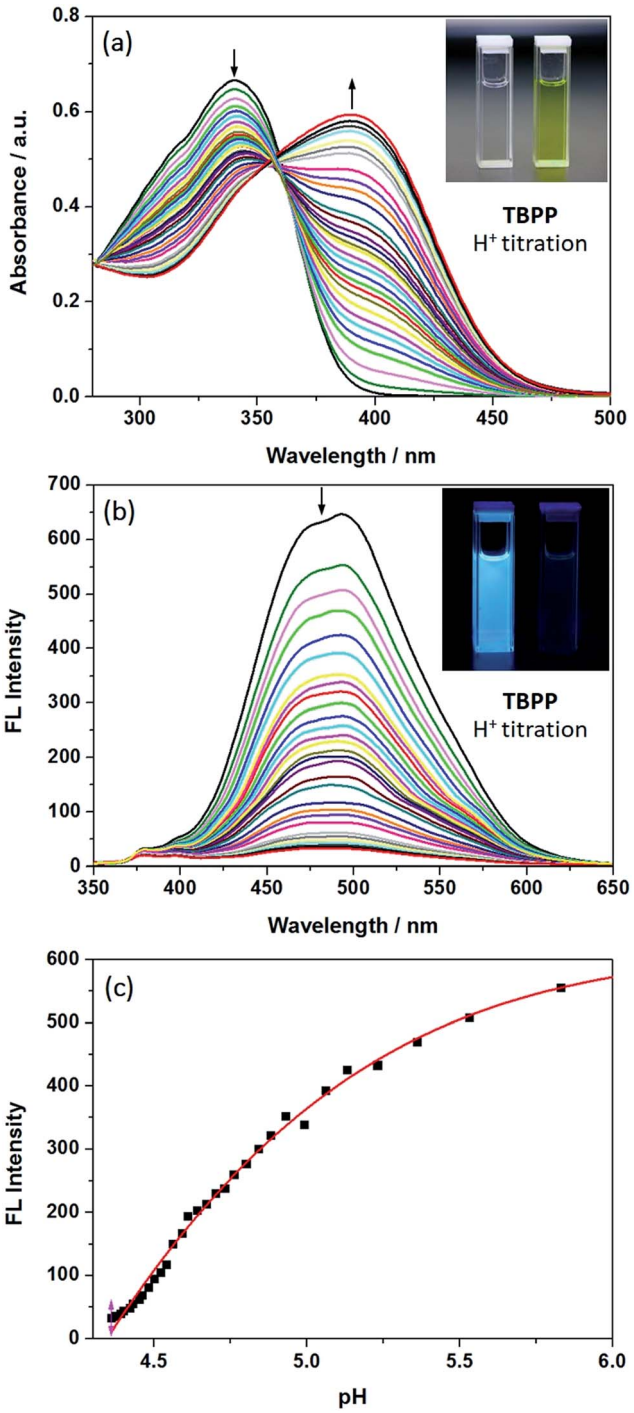

Fig. 2 (a) UV-vis absorption and (b) PL spectra of **TBPP** in DMSO with different pH value. (c) Plots of FL peak intensities of **TBPP** *vs.* pH value. The excitation wavelength is 340 nm. Insert: photos of **TBPP** under natural light and UV lamp (365 nm) before and after the titration.

change was well demonstrated in the fluorescence photos which were shown in the inset of Fig. 2(b). It is should be noted that there was no spectral shift was observed during the titration experiments. This means the new species resulted from the protonation of N atoms in pyridine group is non-emissive in solution state. This property of **TBPP-H$^+$** is similar to our previous pyridinium salts.[27,28] The fluorescence color change

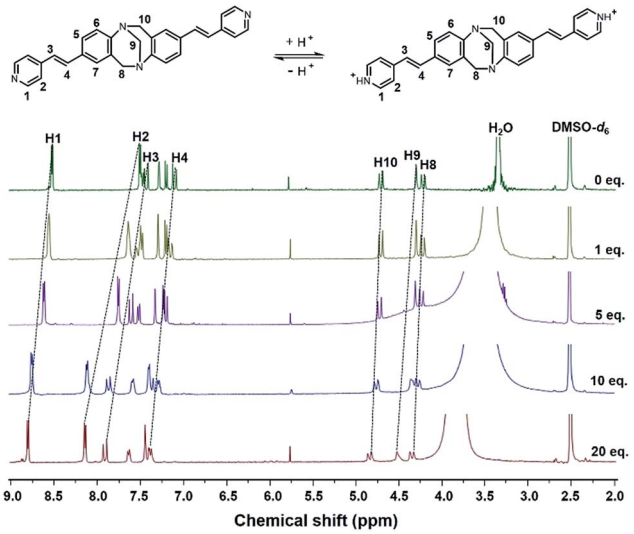

Fig. 3 ^{1}H NMR spectra of probe **TBPP** in DMSO-d_6 and probe with different equivalent hydrochloric acid.

was due to the protonation of N atoms in pyridine group. Under strongly acid condition, the protonation of N atoms in pyridine group enhanced their electron withdrawing ability, which resulted in the of ICT effect from pyridine group to amine group. The structures of **TBPP**, **TBPP-H$^+$** and the sensing process were depicted in Fig. 3. The UV-vis absorption and corresponding fluorescence emission properties during the pH titrations enable probe **TBPP** to serve as a highly sensitive probe for precisely pH measuring in acidic regions through colorimetric and fluorimetric changes.

Proposed mechanism

To study the proton-binding behavior, the ^{1}H NMR spectroscopy of probe **TBPP** in DMSO-d_6 with different equivalent hydrochloric acid has been acquired. As illustrated in Fig. 3, with the addition of incremental amounts of HCl to **TBPP** solution in DMSO-d_6, the pyridine proton signals (H1 and H2) were gradually shifted down-field because of the transformation of the pyridine ring in **TBPP** to an electron-deficient pyridinium unit in **TBPP-H$^+$**. The resonances of phenyl and vinyl protons (H3 and H4) also move to lower fields for the same reason. However, the chemical shifts of amine protons had almost no change (H8, H9 and H10), which indicated that the protonation occurred at the pyridine N rather than amine N. The downfield chemical shift of these protons was obviously due to H^+ binding with N atom of pyridine, which resulted in the decrease of electron density around these protons. The presence of acid–base equilibrium between the two forms of **TBPP** was given in Scheme 2.

Selectivity of probe TBPP

The selectivity response of probe to H^+ over various metal ions were examined at pH 5.83 and 4.10, respectively. It is noteworthy that **TBPP** shows high selectivity toward H^+. As shown in Fig. 4, physiologically ubiquitous metal ions including Na^+, K^+, Mg^{2+} and Ca^{2+}, as well as other heavy and transition metal ions, such

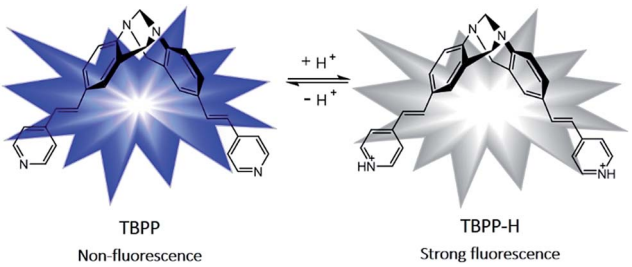

Scheme 2 pH-Dependent equilibrium of probe **TBPP**.

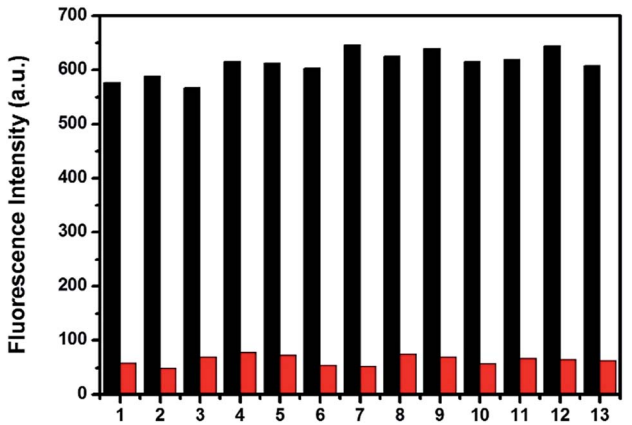

Fig. 4 Fluorescence responses (490 nm) of **TBPP** (10.0 μM) in DMSO solutions at pH 5.83 (black bars) and 4.10 (red bars) in the presence of diverse metal ions. (1) Blank; (2) Na^+ (150 mM); (3) K^+ (150 mM); (4) Ca^{2+} (10 mM); (5) Mg^{2+} (2 mM); (6) Cu^{2+} (0.2 mM); (7) Mn^{2+} (0.2 mM); (8) Co^{2+} (0.2 mM); (9) Ni^{2+} (0.2 mM); (10) Cd^{2+} (0.2 mM); (11) Al^{3+} (0.2 mM); (12) Zn^{2+} (0.2 mM); (13) Cr^{3+} (0.2 mM); the excitation wavelength is 340 nm.

as Cu^{2+}, Mn^{2+}, Co^{2+}, Ni^{2+}, Cd^{2+}, Al^{3+}, Zn^{2+} and Cr^{3+} caused no visible effect on the fluorescence intensity of the probe at pH 5.83 and 4.10. These results revealed that **TBPP** showed an excellent selectivity response to H^+ in the presence of metal ions.

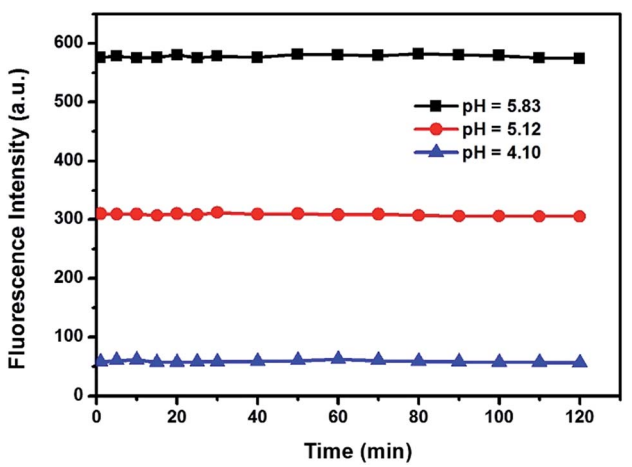

Fig. 5 Changes in the fluorescence intensity at 490 nm for **TBPP** (10.0 μM) in DMSO solutions with times at pH 5.83, 5.12 and 4.10, respectively.

Photostability of probe TBPP

The stability of the probe was tested by measuring the fluorescent response during 2 h with pH 5.83, 5.12, and 4.10, respectively (Fig. 5). The fluorescence intensity was continuously monitored and recorded at set time intervals at 490 nm. The results indicated that the probe can instantly respond to the change of H^+ concentration, and the probe solution is stable. Thus, the probe can be used to monitor the pH variation in real time.

Conclusion

In summary, we have designed and synthesized a new pH fluorescent probe **TBPP** based on TB by introducing the pyridine electron-withdrawing group into TB framework. The UV-vis absorption and fluorescence titrations indicated that **TBPP** can serve as a highly sensitive probe for pH measuring in acidic regions through colorimetric and fluorimetric changes. Furthermore, the detection mechanism has been verified by ^{1}H NMR spectroscopy. The large Stokes shift (149 nm), high sensitivity, good selectivity, and extremely short response time under extreme acidic condition of the probe makes it an extremely effective pH sensor. We believe it will be great beneficial to study chemical and biological system.

Conflicts of interest

There are no conflicts to declare.

Acknowledgements

We gratefully acknowledge the financial support from the state National Natural Science Foundation of China (Grant No. 51403157, 61704128) and the Fundamental Research Funds for the Central Universities.

Notes and references

1 Q. J. Ma, H. P. Li, F. Yang, J. Zhang, X. F. Wu, Y. Bai and X. F. Li, *Sens. Actuators, B*, 2012, **166**, 68.
2 N. I. Georgiev, R. Bryaskova, R. Tzoneva, *et al.*, *Bioorg. Med. Chem.*, 2013, **21**, 6292.
3 X. J. Cao, L. N. Chen, X. Zhang, *et al.*, *Anal. Chim. Acta*, 2016, **920**, 86.
4 X. F. Zhang, T. Zhang, S. L. Shen, *et al.*, *J. Mater. Chem.*, 2015, **3**, 3260.
5 W. Pan, H. Wang, L. Yang, Z. Yu, N. Li and B. Tang, *Anal. Chem.*, 2016, **88**, 6743.
6 J. H. Cheng, Y. H. Zhang, X. F. Ma, X. G. Zhou and H. F. Xiang, *Chem. Commun.*, 2013, **49**, 11791.
7 M. Chesler, *Physiol. Rev.*, 2003, **83**, 1183.
8 A. M. Paradiso, R. Y. Tsien and T. E. Machen, *Nature*, 1987, **325**, 447.
9 R. G. Zhang, S. G. Kelsen and J. C. Lamanna, *J. Appl. Physiol.*, 1990, **68**, 1101.
10 J. Han and K. Burgess, *Chem. Rev.*, 2010, **110**, 2709.
11 J. Yin, Y. Hu and J. Yoon, *Chem. Soc. Rev.*, 2015, **44**, 4619.
12 Y. K. Yue, F. J. Huo, S. Y. Lee, C. X. Yin and J. Y. Yoon, *Analyst*, 2017, **142**, 30.
13 S. He, R. P. Mason, S. Hunjan, V. D. Mehta, V. Arora, R. Katipally, P. V. Kulkami and P. P. Antich, *Bioorg. Med. Chem.*, 1998, **6**, 1631.
14 S. J. Hesse, G. J. Ruijter, C. Dijkema and J. Visser, *J. Biotechnol.*, 2000, **77**, 5.
15 M. J. Kiani, M. A. A. Razak, F. K. C. Harun, M. T. Ahmadi and M. Rahmani, *J. Nanomater.*, 2015, **2015**, 1.
16 J. Zhou, L. Zhang and Y. Tian, *Anal. Chem.*, 2016, **88**, 2113.
17 G. Mattock and G. R. Taylor, *pH Measurement and Titration*, Macmillan, Heywood, London, 1961, vol. 888, p. 31.
18 X. Xiong, F. Song, J. Wang, Y. Zhang, Y. Xue and L. Sun, *J. Am. Chem. Soc.*, 2014, **136**, 9590.
19 Y. H. Chan, C. Wu, F. Ye, Y. Jin, P. B. Smith and D. T. Chiu, *Anal. Chem.*, 2011, **83**, 1448.
20 L. Long, Y. Wu, L. Wang, A. Gong, R. Hu and C. Zhang, *Anal. Chim. Acta*, 2016, **908**, 1.
21 M. Lee, N. G. Gubernator, D. Sulzer and D. Sames, *J. Am. Chem. Soc.*, 2010, **132**, 8828.
22 H. Zhu, J. Fan, Q. Xu, *et al.*, *Chem. Commun.*, 2012, **48**, 11766.
23 L. B. Xu, S. G. Wei, Q. P. Diao, P. Y. Ma, X. Liu, Y. Sun, D. Q. Song and X. H. Wang, *Sens. Actuators, B*, 2017, **246**, 395.
24 J. Tröger, *J. Prakt Chem.*, 1887, **36**, 225.
25 C. X. Yuan, Q. Xin, H. J. Liu, L. Wang, M. H. Jiang and X. T. Tao, *Sci. China: Chem.*, 2011, **54**, 587.
26 V. R. Ögmundur, A. Josep and W. Kenneth, *Eur. J. Org. Chem.*, 2012, 7015.
27 C. X. Yuan, X. T. Tao, Y. Ren, Y. Li, J. X. Yang, W. T. Yu, L. Wang and M. H. Jiang, *J. Phys. Chem. C*, 2007, **111**, 12811.
28 C. X. Yuan, X. T. Tao, L. Wang, J. X. Yang and M. H. Jiang, *J. Phys. Chem. C*, 2009, **111**, 6809.
29 Z. Y. Yang, W. Qin, W. Y. Lam, S. J. Chen, H. Y. Sung, D. Williams and B. Z. Tang, *Chem. Sci.*, 2013, **4**, 3725.
30 J. B. Chao, H. J. Wang, Y. B. Zhang, C. X. Yin, F. J. Huo, K. L. Song, Z. Q. Lia, T. Zhang and Y. Q. Zhao, *Talanta*, 2017, **174**, 468.
31 J. Jensen, M. Strozyk and K. Wärnmark, *J. Heterocycl. Chem.*, 2003, **40**, 373.
32 P. Fromherz, *J. Phys. Chem.*, 1995, **99**, 7188.
33 U. Narang, C. F. Zhao, J. D. Bhawalkar, F. V. Bright and P. N. Prasad, *J. Phys. Chem.*, 1996, **100**, 4521.
34 J. Chao, H. Wang, K. Song, Z. Li, Y. Zhang, C. Yin, F. Huo, J. Wang and T. Zhang, *Tetrahedron*, 2016, **72**, 8342.
35 F. Miao, G. Song, Y. Sun, Y. Liu, F. Guo, W. Zhang, M. Tian and X. Yu, *Biosens. Bioelectron.*, 2013, **50**, 42.